Article

Drug-Containing Layered Double Hydroxide/Alginate Dispersions for Tissue Engineering

Juan Pablo Zanin [1,2,3,4], German A. Gil [3,4], Mónica C. García [5,6] and Ricardo Rojas [1,2,*]

1   Departamento de Fisicoquímica, Facultad de Ciencias Químicas, Universidad Nacional de Córdoba, Córdoba 5000, Argentina
2   Consejo Nacional de Investigaciones Científicas y Técnicas, CONICET, Instituto de Investigaciones en Fisicoquímica de Córdoba, INFIQC, Córdoba 5000, Argentina
3   Departamento de Química Biológica, Facultad de Ciencias Químicas, Universidad Nacional de Córdoba, Córdoba 5000, Argentina
4   Consejo Nacional de Investigaciones Científicas y Técnicas, CONICET, Centro de Investigaciones en Química Biológica de Córdoba, CIQUIBIC, Córdoba 5000, Argentina
5   Departamento de Ciencias Farmacéuticas, Facultad de Ciencias Químicas, Universidad Nacional de Córdoba, Córdoba 5000, Argentina
6   Consejo Nacional de Investigaciones Científicas y Técnicas, CONICET, Unidad de Investigación y Desarrollo en Tecnología Farmacéutica, UNITEFA, Córdoba 5000, Argentina
*   Correspondence: ricardo.rojas@unc.edu.ar

Abstract: Alginate (Alg) is increasingly studied as a constitutive material of scaffolds for tissue engineering because of its easy gelation and biocompatibility, and the incorporation of drugs into its formulation allows for its functionality to be extended. However, Alg presents a low cell adhesion and proliferation capacity, and the incorporation of drugs may further reduce its biocompatibility. Layered double hydroxides (LDH) are promising fillers for Alg-based biomaterials, as they increase cell adhesion and interaction and provide drug storage and controlled release. In this work, LDH containing ibuprofen or naproxen were synthesized by coprecipitation at a constant pH and their properties upon their incorporation in Alg dispersions (LDH-Drug/Alg) were explored. Drug release profiles in simulated body fluid and the proliferation of pre-osteoblastic MC3T3-E1 cells by LDH-Drug/Alg dispersions were then evaluated, leading to results that confirm their potential as biomaterials for tissue engineering. They showed a controlled release with diffusive control, modulated by the in-situ formation of an Alg hydrogel in the presence of Ca^{2+} ions. Additionally, LDH-Drug/Alg dispersions mitigated the cytotoxic effects of the pure drugs, especially in the case of markedly cytotoxic drugs such as naproxen.

Keywords: scaffolding biomaterials; drug delivery systems; hydrogel; cytotoxicity

1. Introduction

Alginate (Alg) is a natural polymer that is extensively used in drug delivery and scaffolding applications. It is composed by monomers of α-L-guluronate and β-D-mannuronate in a ratio that varies depending on the type of seaweed from which it is extracted. Alg presents a high concentration of carboxylate groups that are charged at pH values above 3–4, being highly soluble under neutral and alkaline conditions. Alg is cross-linked by Ca^{2+} ions (Ba^{2+} and Zn^{2+} ions are also used to a lesser extent) to form hydrogels [1]. Alg is commonly used as excipient in the pharmaceutical industry, but it has also been used as a drug carrier, providing increased drug solubility, pH-triggered and/or controlled release rate [2]. More recently, Alg has been proposed for tissue engineering applications due to its similarity to other extracellular matrix components, as well as its biocompatibility, gel-forming ability, and water retention capacity, thus providing a suitable environment for the regeneration of tissues and organs, such as skeletal bone, skin, nerve, liver, and pancreas [3]. Particularly, Alg is extensively used to fabricate scaffolds for bone tissue engineering, either alone or

in combination with other polymers, either hydrophilic (i.e., chitosan) or hydrophobic (i.e., polylactic acid and polycaprolactone), as well as (nano)particles [4–6]. Strategies such as cell seeding, and drug delivery have been applied to such scaffolds to expand and to optimize their bio-functionality.

Nevertheless, the applications of Alg in tissue engineering are hindered by its poor mechanical properties and low capacity for cell adhesion and proliferation. Furthermore, the leakage of drug loading during cross-linking of the Alg matrix and fast drug release under biological conditions decrease the effectiveness of approaches involving the incorporation of drugs and biomolecules [7,8]. Particles, particularly those of an inorganic nature, such as hydroxyapatite, graphene, clay and layered double hydroxides (LDH) have been used to reinforce the mechanical properties of Alg, increase its bifunctionality and control the release of the drugs included its formulations [9].

LDH are bidimensional solids with brucite ($Mg(OH)_2$)-like layers that present the isomorphic substitution of divalent by trivalent ions, which leads to anion intercalation and exchange capacity. LDH present a great versatility and customization capacity due to the different metal ions (either divalent or trivalent) that can be included in their layers, as well as their anion exchange and surface adsorption properties [10]. LDH, due to their lamellar structure and anion exchange capacity, as well as their biocompatibility and ability to interact with cells, are also extensively used for tissue engineering applications [11,12]. They also present the high drug loading capacity of acidic drugs between their layers, and have been proposed as nanocarriers for cell internalization and the release of drugs and genes. In this sense, several types of drugs have been intercalated into LDH interlayers, among which nonsteroidal anti-inflammatory drugs (NSAID) have shown a controlled release rate and improved solubility in acid media [13–17].

Due to the carboxylate anions in its structure, Alg presents electrostatic interactions with positive LDH surface charges. As a result, LDH particles attach to Alg chains [18,19], being retained upon the formation of Alg-Ca hydrogels [20]. LDHs intercalated with NSAID such as ibuprofen (Ibu), diclofenac and naproxen (Nap) have also been incorporated into Alg composites, and beads [7,21,22]. Silver sulfadiazine-loaded LDH have also been incorporated into Alg films [23] for wound-dressing applications. The inclusion of LDH particles produced controlled drug release and sustained antimicrobial activity while maintaining a low cytotoxicity in cells. Nevertheless, the drug release under body conditions, especially for non-gelled LDH/Alg dispersions, has scarcely been explored, and LDH's effect on the cytotoxicity of both Alg and the incorporated drugs is also poorly explored. These aspects are essential for their performance as biomaterials for tissue engineering, with non-gelled dispersions being especially suitable, as they allow for the easy incorporation of cells, allowing for a posterior in-situ gelation.

In this work, we prepared drug-loaded LDH (LDH-Drug) particlesin Alg dispersions (LDH-Drug/Alg) and explored their release performances and biocompatibility as scaffolding biomaterials for tissue engineering. With this aim, Mg-Al LDH intercalated with Ibu and Nap was synthesized by coprecipitation at a constant pH, and its properties upon incorporation in Alg dispersion were explored. The release profiles of intercalated drugs toward bio-relevant fluids and the proliferation capacity of these biomaterials were evaluated against pre-osteoblastic MC3T3-E1 cell cultures.

2. Materials and Methods

Ibu and Nap anhydrous acids (≥98% purity, Parapharm®), $MgCl_2 \cdot 6H2O$ (Baker®), $AlCl_3 \cdot 6H2O$ (Anedra®), NaOH (Baker®), NaOH granules (PA grade, Cicarelli®), 37% w w^{-1} HCl solution (PA grade, Cicarelli®), KH_2PO_4 and K_2HPO_4 (PA grade, Anedra®), NaCl (PA grade, Cicarelli®), $NaHCO_3$ (PA grade, Cicarelli®), KCl (PA grade, Anedra®), (PA grade, Cicarelli®), tris (hydroxymethyl)aminomethane (Tris buffer, PA grade, Biopack®), and Na_2SO_4 (PA grade, Baker, polyacrylate (PA, 40% w/w solution, molecular weight, MW = 8 kDa, Sigma Aldrich). Minimum Essential Medium Eagle without ascorbic acid (MEM, Thermo Fisher, Waltham, MA, USA), fetal bovine serum (FBS, Gibco/Thermo Fisher), Penicillin-

Streptomycin-Neomycin (PSN) Antibiotic Mixture (Thermo Fisher) and alamarBlue (Merck). Phosphate buffer solution (PBS) at pH 7.4 was prepared according to USP specifications [24]. Simulated body fluid (SBF) was prepared according to standardized parameters [25].

Deionized water (18 MΩ MilliQ, Millipore® System) was used in all experiments, which were conducted at room temperature (25 °C) unless otherwise stated.

2.1. Synthesis and Structural Characterization of LDH-Drug

Mg-Al LDH loaded with NSAID (LDH-Drug, either LDH-Ibu or LDH-Nap) were synthesized by the coprecipitation method at constant pH. A solution of the metal ions (0.4 mol L^{-1} AlCl$_3$ and 1.2 mol L^{-1} MgCl$_2$, 0.1 L) was added to a 0.1 L solution containing 0.06 mol of the corresponding drug, previously dissolved by addition of NaOH. The addition was performed dropwise, under constant stirring, in nitrogen atmosphere and at pH = 9, controlled by addition of a 2.0 mol L^{-1} NaOH solution. The addition of this solution was controlled by a Titrando 905 automatic titrator (Metrohm) coupled to a Metrohm 9.0262.100 combined pH electrode. The obtained slurries were centrifuged, washed, and finally dried at 50 °C until constant weight. For cell proliferation studies, a LDH intercalated with chloride (LDH-Cl) was synthesized with the same procedure, but replacing the drug with NaCl.

The powder X-ray diffraction (PXRD) patterns were recorded with a Phillips X'pert Pro instrument equipped with a Pixcell 1D detector and a CuKα lamp (λ = 1.5408 Å) at 40 kV and 40 mA. The scans were performed in continuous mode (10° min^{-1}) between 5 and 70°. Low angle measurements (2–10°) were performed in step mode (0.05°, 1.2 s) with a Xe detector coupled to a graphite monochromator. Fourier-transform infrared (FTIR) spectra were measured with a FTIR Bruker IFS28 instrument using KBr pellets (1:200 sample:KBr ratio) at a 4 cm^{-1} resolution and accumulating 32 scans. Scanning electron microscopy (SEM) images were obtained in a FE-SEM Σigma instrument on samples covered with a Cr layer. The Mg/Al ratio was determined by energy dispersive X-ray spectroscopy (EDS) in the same instrument. The drug content of the samples was determined in dispersions of samples (1 g L^{-1}) prepared in PBS, which were equilibrated until a constant drug concentration was reached. The drug concentration in the supernatants was determined by UV-Vis spectrophotometry (Agilent Technologies® Cary 60) at λ = 222 nm (Ibu) and 272 nm (Nap).

2.2. Dispersion of LDH–Drug Particles

The dispersion of the dried LDH–drug particles was essayed in different media and under different conditions to optimize their interaction with Alg and determine the effect on the particle distribution. Both LDH-Ibu and LDH-Nap (5 g L^{-1}), alone or together with Alg powder (2 % w w^{-1}), were dispersed in water and equilibrated for 24 h. These dispersions were then sonicated for 2 h and sterilized in an autoclave at 121 °C. Aliquots of the dispersions were taken after the sonication and the autoclave step and diluted 1:10 in water. The hydrodynamic apparent diameter (d) and zeta potential (ζ) of LDH–drug particles were determined by dynamic light scattering (DLS) and electrophoretic light scattering (ELS) measurements, respectively, using a Delsa Nano C instrument (Beckman Coulter). Drug released from LDH in Alg dispersions was determined after sonication and thermal treatment (TT). The dispersions were centrifuged and filtered and the free drug concentration in the supernatants was determined as previously described. A dispersion of the LDH–drug particles in a 2% polyacrylate (MW = 8 kDa) equilibrated for 24 h without further treatment was used for comparative purposes.

2.3. In Vitro Drug Release Studies

Release studies of both Ibu and Nap from 2% Alg dispersions of LDH–drug particles at two different concentrations (0.5 and 5 g L^{-1}, prepared as described in Section 2.3) were performed in bicompartmental diffusion devices (Franz cells). A semisynthetic acetate cellulose membrane (molecular cut-off 12 kDa, Sigma-Aldrich®) was mounted between the

donor and the receptor compartments. The release profiles from 2% Alg dispersions with equivalent concentrations of the pure drugs were also analyzed. A total of 1 mL of each sample was carefully placed in the donor compartment and kept in contact with 16.5 mL of receptor medium (PBS and SBF) at 37.0 ± 0.5 °C. 1 mL aliquots of receptor medium were withdrawn at predetermined time intervals (5; 15; and 30 min; 1; 1,5; 2; 3; 4; 5; 6; 7; and 8 h) and replaced with equivalent volumes of preheated fresh medium. The concentration of each drug was determined by UV-Vis spectrophotometry as previously described, using calibration curves constructed for each drug at each receptor medium. All experiments were conducted in triplicate and the sink conditions were maintained.

The drug release profiles were statistically compared using the difference factor (f_1) and the similarity factor (f_2) (Equations (1) and (2), respectively). According to this methodology, an f_1 value above 15 and an f_2 value in the 0–49 range implies a difference between the release profiles [26].

$$f_1 = \frac{\sum_{t=1}^{n} |R_t - T_t|}{\sum_{t=1}^{n} Rt} \times 100 \tag{1}$$

$$f_2 = 50 \, log \left\{ \left[1 + \frac{1}{n} \sum_{t=1}^{n} (R_t - T_t)^2 \right]^{-0.5} \right\} \times 100 \tag{2}$$

where R_t and T_t are the cumulative percentages of drug released at each of the n time points of the reference and test sample, respectively.

The release profiles were fitted with common mathematical models [26]:

Zero order:

$$\% \, Drug = \% \, Drug_0 + k_Z t \tag{3}$$

Higuchi:

$$\% \, Drug = \% \, Drug_0 + k_H t^{0.5} \tag{4}$$

Korsmeyer–Peppas (K-P):

$$\% \, Drug = \% \, Drug_0 + k_P t^{n} \tag{5}$$

where $\% \, Drug_0$ is the intercept, often referring to the initial amount of drug in the receptor or fast processes that are produced at the beginning of the release experiment (*burst* effect). k_0, k_H and k_P are the kinetic constants corresponding to zero-order, Higuchi, and K-P kinetic models, respectively. Finally, n parameter in the K-P model (Equation (5)) describes the release mechanism: when $n = 0.5$, the fraction of drug released is proportional to the square root of time (Higuchi model, Equation (4)) and the drug release is purely diffusion controlled; while, when $n = 1$, the equation is identical to that of zero-order (case-II transport, Equation (3)). Values of n between 0.5 and 1 indicate an anomalous process with contributions from different phenomena, such as ionic exchange and the relaxation of polymer chains, among others.

2.4. Cell Proliferation Assay

MC3T3-E1 cells were maintained in a complete medium (CM) prepared with MEM, 10% FBS, and 1 × PSN antibiotics at 37 °C in 5% CO_2 atmosphere. An MC3T3-E1 cell line was obtained from ATCC (Manassas, VA, USA) in 2020, cultured at 37 °C in 5% CO_2 atmosphere until passage 2–4, and then cultured for 3–4 additional passages if necessary. Cells were authenticated based on morphology and growth curve analysis. Mycoplasma detection was performed every 2 months by PCR and Hoechst 33,258 staining [27].

Cell proliferation was assessed using alamarBlue, a resazurin-based solutions (fluorometric/colorimetric) growth indicator that changes from an oxidized (nonfluorescent, blue) form to a reduced (fluorescent, red) form when reduced by mitochondrial respiration. Cells were seeded in 96-well plates (3000 cells/well) and maintained for 1 day until complete cell attachment. The growth medium was then discarded and replaced with medium containing the different samples, and 10% alamarBlue was added. Treated cells were

incubated for 24 and 48 h and the fluorescence intensity was measured on a PlateReader (Biotek[®], excitation/emission = 535 nm/590 nm). The performed tests were control (pure CM); Alg; LDH; LDH-Cl/Alg; pure drug (anionic); Drug/Alg; 5 g L^{-1} LDH-Drug; and 5 g L^{-1} LDH-Drug/Alg. The concentration of LDH-Cl and drug used for each control were equivalent to the amount contained in the 5 g L^{-1} LDH-Drug/Alg dispersions, while Alg concentration was 2% in all cases. The results were expressed as a percentage of the intensity recorded for the corresponding control experiment.

Data are expressed as mean $\pm$ standard deviation (SD) (n = 4). Statistical significance of comparisons of mean values was assessed by two-way ANOVA test, followed by Tukey's multiple comparison. p values above 0.05 were considered statically significant.

3. Results and Discussion

3.1. Structural Characterization of the LDH–Drug Samples

The proposed synthesis was effective in obtaining LDH phases that were completely intercalated with the corresponding drug. The PXRD patterns of the samples (Figure 1a) showed narrow and intense peaks corresponding to the (0 0 l) reflections of LDH structure at 2θ values lower than 30°. Wide and asymmetric peaks corresponding to (0 1 l) reflections and a peak due to a (1 1 0) plane were obtained at larger 2θ values. This last peak allowed for the *a* parameter of the rhombohedral cell of LDH structure (Table 1) to be obtained, which was similar to that commonly obtained for LDH phases in both cases [28] and to that obtained for the reference sample LDH-Cl. The (0 0 l) peaks were recorded at low 2θ, corresponding to the LDH intercalated with large anions, and led to large values of the *c* cell parameter, while LDH-Cl showed (0 0 l) peaks at larger 2θ values. The interlayer distances (c/3 = 22.2 and 22.4 Å for LDH-Ibu and LDH-Nap, respectively) gave a hint of the drug disposition between the layers. Thus, the Ibu anion presents a length, at its larger axis, of around 9.7 Å [29], which led to a theoretical interlayer distance (accounting on a 4.8 Å for the layer height) of 14.5 Å for a perpendicular, monolayer arrangement and 24.3 Å for a bilayer one. However, the most common values are around 22.5 Å, which was assigned to a tilted bilayer disposition that maximizes the interaction between carboxylate anions and the hydroxyl anions of the layers [29]. Although Nap is a larger anion (its length is around 12 Å), the interlayer spacings obtained for LDH-Nap are quite close to that of LDH-Ibu [30,31]. These lower spacings indicate that a higher tilting from a perpendicular arrangement to the LDH layers is produced for this anion.
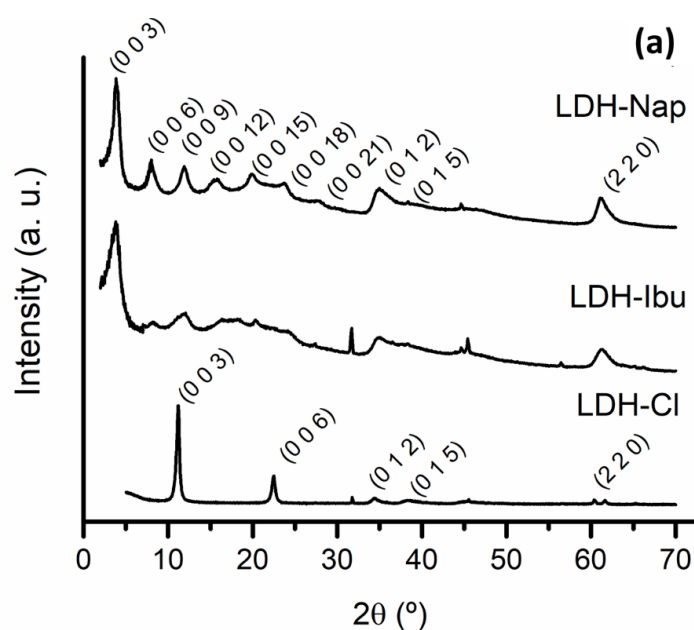

Figure 1. *Cont.*
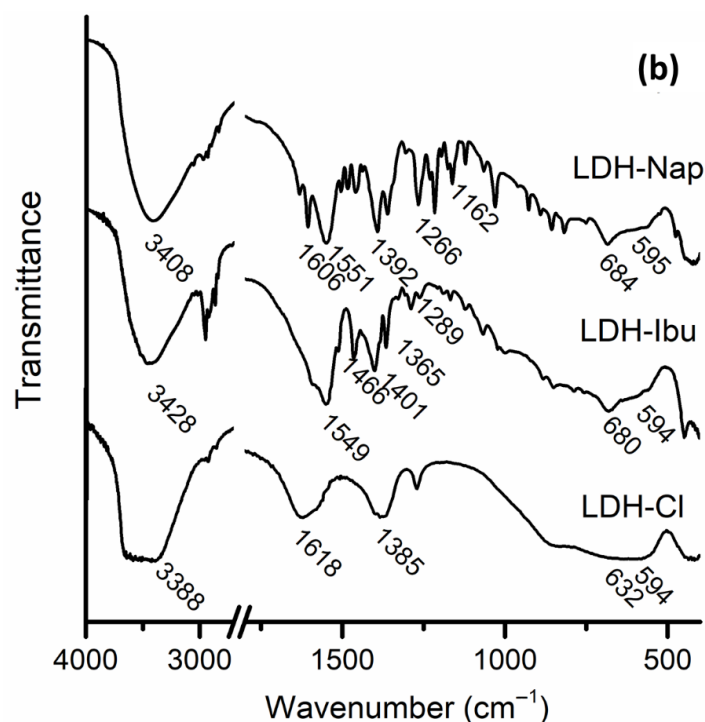
Figure 1. FT-IR spectra (**a**) and PXRD patterns (**b**) of LDH-Cl, LDH-Ibu and LDH-Nap samples.

Table 1. Chemical analysis and proposed formula for the synthesized LDH–drug samples.

Sample	% Mg	% Al	% D	% H$_2$O *	Chemical Formula	a(Å)	c (Å)
LDH-Ibu	11.3	6.5	47.9	9.5	Mg$_{0.66}$Al$_{0.34}$(OH)$_2$Ibu$_{0.34}$· 0.75 H$_2$O	3.02	66.5
LDH-Nap	12.2	6.2	46.9	9.3	Mg$_{0.69}$Al$_{0.31}$(OH)$_2$Nap$_{0.31}$· 0.72 H$_2$O	3.02	67.3

* Obtained from the weight loss at 200 °C.

The FT-IR spectra showed characteristic peaks in both the LDH structure and the intercalated drugs (Figure 1b). The band centered at 3428 and 3408 cm^{-1} for LDH-Ibu and LDH-Nap, respectively, was assigned to the O-H stretching mode (ν_{OH}) of OH$^-$ anions and H$_2$O water molecules. The bands recorded at wavenumbers below 1000 cm^{-1}, especially those at 594–595 cm^{-1}, were assigned to the lattice vibrations of the LDH layers [32,33]. The band corresponding to the bending vibration of structural water molecules between the layers registered at 1618 cm^{-1} for LDH-Cl was missing for LDH–drug samples due to the strong drug bands in the 1550–1650 cm^{-1} region. These bands were assigned to the ν_{asym} (at 1549 and 1551 cm^{-1} for LDH-Ibu and LDH-Nap, respectively) and ν_{sym} (1401 and 1392 cm^{-1}) of the carboxylate anions of the intercalated drugs. The difference between the maxima of these bands ($\Delta\nu = \nu_{asym} - \nu_{sym}$) is considered to be indicative of the interactions established between the carboxylate group and the hydroxylated layers [34]. The obtained values (148 and 159 cm^{-1} for LDH-Ibu and LDH-Nap, respectively) corresponded to weak interactions produced by electrostatic forces between the negatively charged carboxylate groups and the positively charged layers, as well as the hydrogen bonding between these groups and the hydroxyl anions of the layers. Other characteristic bands were registered at 1466 and 1365 cm^{-1} (δ (CH$_2$)) and at 1289 cm^{-1} (γ (OH)) for LDH-Ibu [35,36] and at 1266 (ν (C-O)), 1162 (ν (C-O-C)) and 1606 (aromatic ring) for LDH-Nap, among others [37,38]. Neither of the samples presented C = O stretching vibrations characteristic of the carboxylic group, which indicated that the acidic form of the drug was negligible in both cases.

Then, a single LDH phase, fully intercalated with the anionic form of the respective drugs, was obtained in both cases, as confirmed by the chemical analysis of the samples

(Table 1). The determined drug content (% D) was consistent with a 100% occupation of the exchange sites of LDH structure. Then, negligible anion excess was detected by the chemical analysis of the samples. Nevertheless, the presence of a slight anion excess in the surface of LDH-Ibu was suggested by the negative ζ of these particles (Figure 2). These values indicated that these anions were attached to LDH layers by specific interactions besides the electrostatic ones. In the case of anions attached exclusively by electrostatic interactions, the ζ values are positive, reversed only at high pH values [39,40]. In previous works, we even found a slight excess of Ibu$^-$ anions, caused by the additional stabilization assigned to hydrophobic interactions between the nonpolar sections of adjacent Ibu$^-$ anions. This excess was not produced for Nap$^-$ anions due to the presence of polar groups in its hydrophobic tail, which weakens the hydrophobic interactions [14,38].
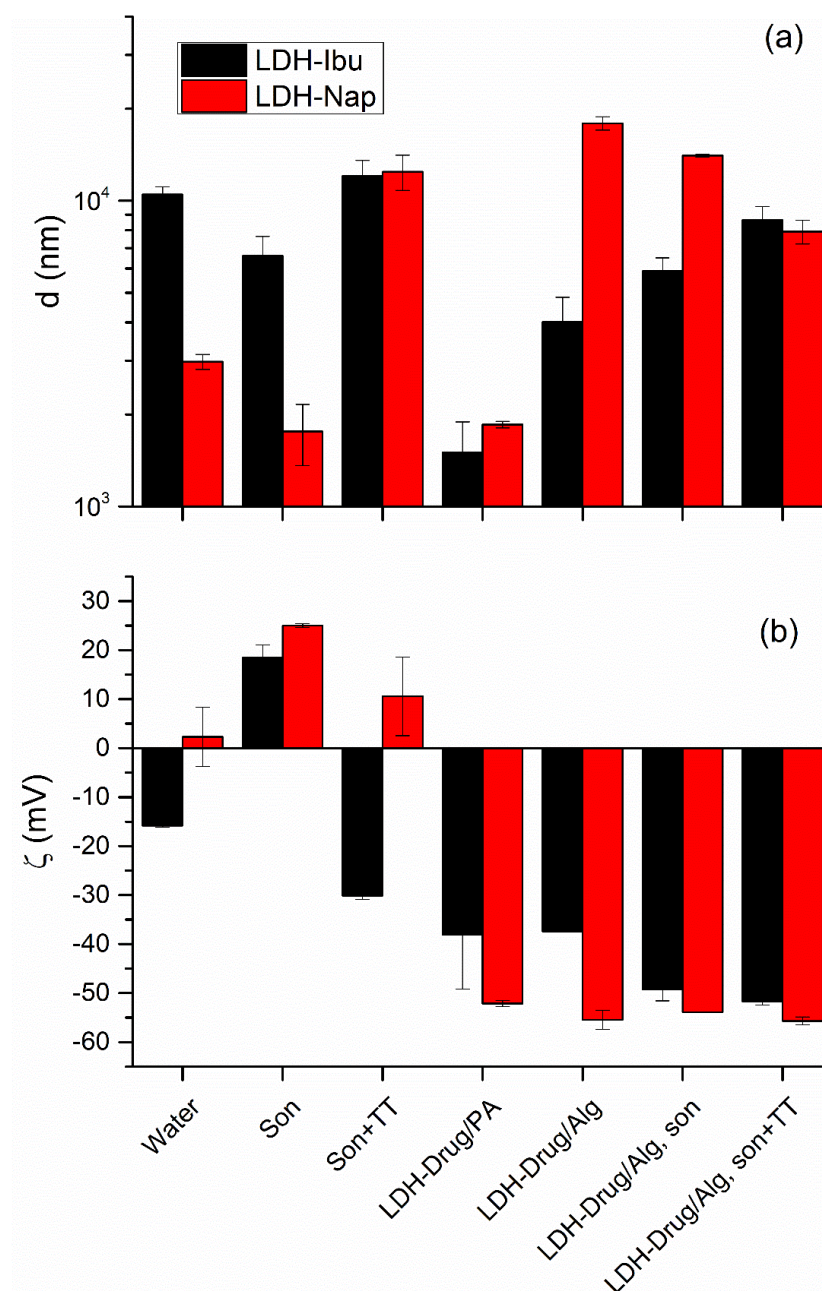

Figure 2. Hydrodynamic apparent diameter, d (**a**) and zeta potential, ζ (**b**) values obtained for LDH-Ibu and LDH-Nap dispersions (1 g L^{-1}) in different media and preparation conditions (son, sonicated; TT, thermal treatment; PA, 2% polyacrylate dispersion).

The morphology of LDH particles and agglomerates was studied using SEM images (Figure 3) and the d values registered by DLS (Figure 2a). The particles of both LDH-Ibu and LDH-Nap were heavily agglomerated, with the size of the agglomerates being larger for the former. Thus, LDH-Ibu particles in the SEM images completely lost the typical lamellar morphology of LDH particles, being merged in agglomerates with rounded edges and smooth surfaces. The size of LDH-Ibu agglomerates was variable, although most samples were above 10 μm, which was in accordance with the d values obtained by DLS measurements. The large aggregation of LDH-Ibu particles was assigned to the hydrophobic surface of the LDH-Ibu particles, as the anion drug is exposes its nonpolar tail to the aqueous side of the interface. Therefore, interactions between hydrophobic LDH particles was favored, while the surface tension with water is increased. The SEM images of LDH-Nap showed more defined particles and less aggregation, in good accordance with the d values obtained by DLS. The lower aggregation of LDH-Nap was assigned to the presence of a polar ether (C-O-C) group at the end of the hydrophobic tail. As a result, the interaction between the LDH-Nap particles is weaker and the surface tension with water is lower, allowing for a better dispersion of their particles and a lower agglomeration.
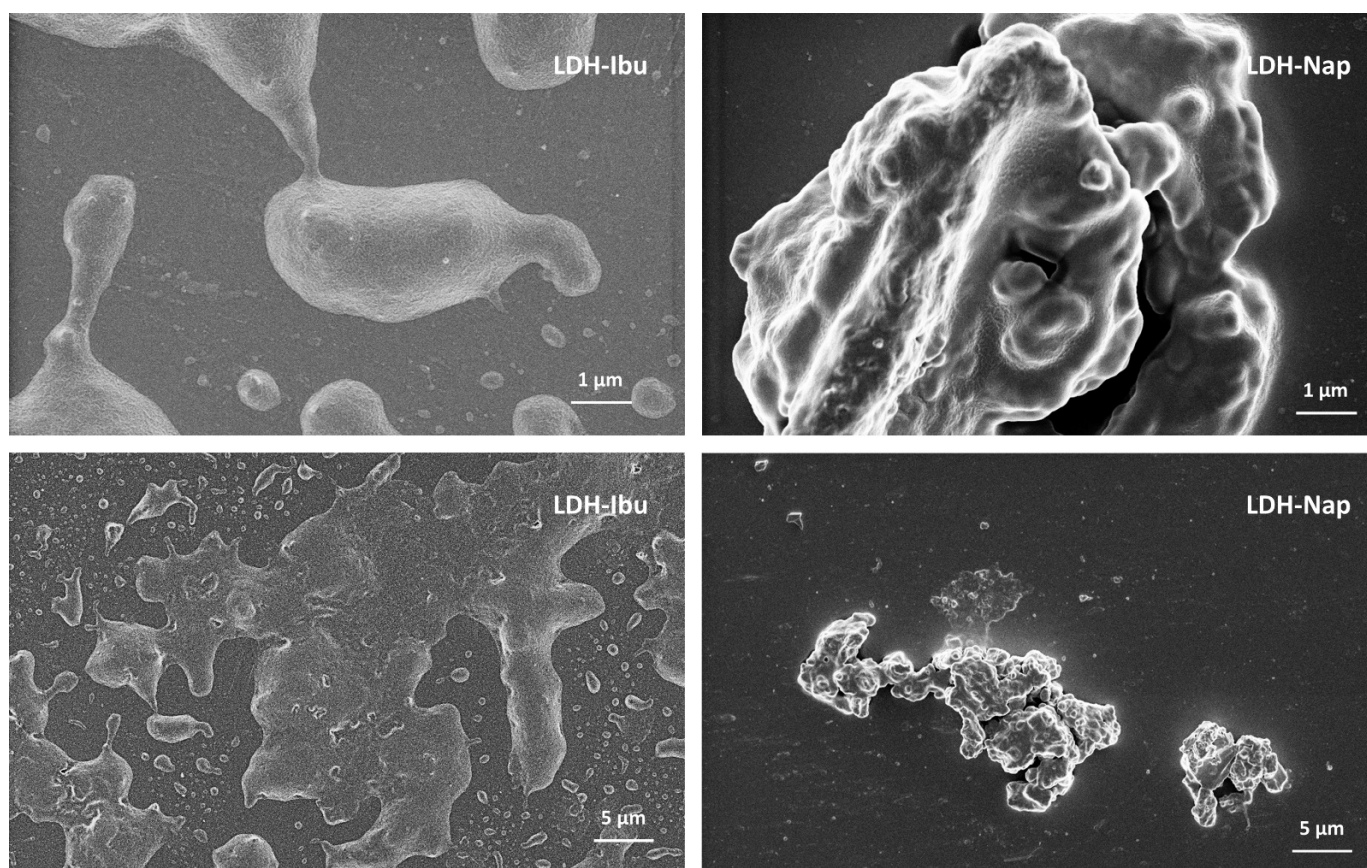

Figure 3. SEM images of LDH–drug samples shown at different magnifications.

3.2. Dispersion of LDH–Drug Particles

Both d and ζ values of the LDH particles were affected by dispersion conditions and the presence of Alg (Figure 2). Thus, the sonication of water dispersions produced a reversal of the ζ values of LDH-Ibu and an increase in the already positive ζ of LDH-Nap, which indicated that drug anions were detached from the particle surface. As a result, the surface hydrophilicity increased, which diminished aggregation, leading to smaller d values. In contrast, the TT sterilization of dispersions produced the opposite effect: the ζ of LDH-Ibu particles was reversed, that of LDH-Nap decreased and the d values of both LDH–drug dispersions increased. Then, the drug adsorption at the surface of LDH formed

an equilibrium that was quite sensitive to the medium conditions, as reflected by the weak interaction of these anions with the particle surface, especially for those incorporated by specific interactions other than the electrostatic.

LDH–drug particles in Alg dispersions (LDH-Drug/Alg) impacted the properties on both d and ζ values. Nevertheless, this impact was greater in the latter, corresponding to polyelectrolytes with a relatively low affinity for LDH surface [19], which was decreased by the affinity and hydrophobic nature of the intercalated drugs. Thus, LDH-Drug/Alg and LDH-Drug/polyacrylate presented large and negative ζ values with relatively minor differences between both electrolytes, which indicated that LDH interacted with both polyelectrolytes. Nevertheless, the Alg interaction with LDH led to large d values in comparison with polyacrylate, which present a larger concentration of carboxylate anions and, consequently, stronger interactions [19,41,42]. Alg, on the other hand, presents a lower density of carboxylate anions, leading to a poor disaggregation in the case of LDH-Ibu/Alg, and even an increased particle size in the case of LDH-Nap/Alg. In the first case, the size diminution was related to the displacement of Ibu⁻ anions of the LDH structure, diminishing the hydrophobicity of the surface, while the increased aggregation in the case of LDH-Nap particles was assigned to the bridging of LDH-Nap particles by Alg chains. In any case, d values for both LDH-Drug/Alg dispersions converged upon sonication and TT and the LDH-Drug/Alg dispersions in these conditions presented only a slightly lower aggregation than dispersions in pure water at the same conditions. Nevertheless, it should be considered that the results present a significant uncertainty, as the equipment used for the measurements presents significant random errors in this size range. Then, although LDH presents an interaction with Alg, this was not strong enough to produce a fine dispersion of the particles, similarly to that previously obtained for LDH-Cl nanoparticles [19]. On the other hand, interaction with a polyelectrolyte such as Alg produces a significant detachment of the drug from the particle surface [42]. Thus, 33% and 35% was released from the LDH in LDH-Ibu/Alg and LDH-Nap/Alg dispersions, respectively (values after sonication and TT).

3.3. In Vitro Drug Release Results

The release behavior of both drugs, Nap and Ibu, from LDH-Drug/Alg dispersions was studied to evaluate their performance as carrier systems (Figure 4). Two different LDH–drug particle concentrations (5 and 0.5 g L⁻¹ LDH-Drug/Alg) were analyzed. The release profiles of Alg dispersions containing the pure drug in its anionic form (Drug/Alg) were obtained at a drug concentration equivalent to that of 0.5 g L⁻¹ LDH-Drug/Alg. The release media were SBF, used to study the apatite-forming ability of implant materials [43], and PBS, a typical release medium to study drug release from delivery systems in simulated plasma conditions.

Controlled release towards both receptor media was achieved, but remarkable differences in the release profiles were observed depending on the release media. Thus, negligible *burst* effects (2.4 and 5.7% of the drug released at t = 15 min for LDH-Ibu/Alg and LDH-Nap/Alg, respectively) were observed toward PBS, lower than that of Drug/Alg (7.5% in both cases). This *burst* effect minimization was even more significant in SBF, in which the percentages of drug released at t = 15 min from 5 g L⁻¹ LDH-Ibu/Alg and LDH-Nap/Alg were 1.5 and 3.2%, while those from Ibu/Alg and Nap/Alg were 13.9 and 12%, respectively.
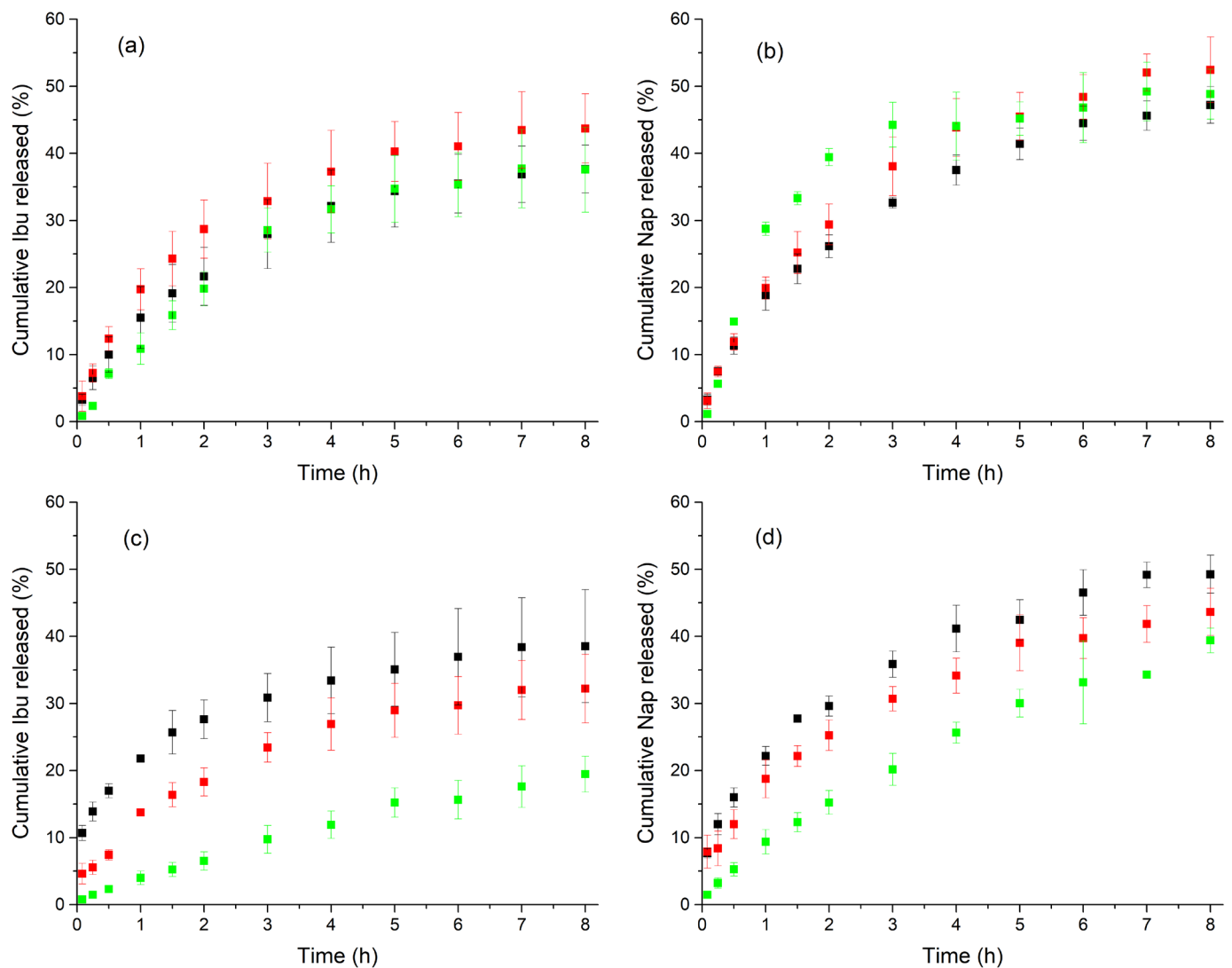
Figure 4. In vitro release profiles), using bicompartmental cells filled with PBS (**a**,**b**) and SBF (**c**,**d**), of Ibu (**a**,**c**) and Nap (**b**,**d**) from LDH-Drug/Alg dispersions at two different concentrations: 5 g L^{-1} (green), and 0.5 g L^{-1} (red), and Alg dispersions with the pure drug at a concentration equivalent to that of 0.5 g L^{-1} LDH-Drug/Alg (black.

For PBS, all release profiles, even those of pure drugs, were similar ($f_2 > 50$); however, the analysis of fitting curves and resulting kinetic parameters (Table 2) established slight but relevant differences. The best fittings were obtained when the K-P model was applied, with n coefficients near 0.5 for the profiles of Drug/Alg and 0. 5 g L^{-1} LDH-Drug/Alg samples and, accordingly, good fittings were also obtained with the Higuchi model. This indicated that the release rate was determined by diffusion processes. Higher n values (0.84 and 0.74 for Ibu and Nap, respectively) and poorer Higuchi fittings were obtained for LDH-Drug/Alg samples at 5 g L^{-1}, which indicate an anomalous behavior, assigned to the combined control of two main mechanisms, drug migration through the Alg dispersion and ion exchange from LDH particles. The main difference was a slightly slower release ($f_1 = 15$) obtained for Ibu (cumulative drug release at the end of the experiment between 38 and 43% in all cases) compared to Nap-containing samples at 0.5 g L^{-1} LDH-Drug/Alg (between 47 and 52%). This difference was related to the higher chemical affinity for the LDH interlayer of Ibu$^-$ anions compared to Nap$^-$ ones [14].

Table 2. Release kinetic data obtained from drug release studies using empirical equations: zero-order, Higuchi and K-P models, fittings with the best R^2 are marked with asterisks.

Sample	Receptor Media	Zero-Order			Kinetic Models Higuchi			Korsmeyer-Peppas		
		% $Drug_0$	k_0	R^2	% $Drug_0$	k_H	R^2	k_P	n	R^2
LDH-Ibu/Alg, 5 g L^{-1}		6.6	4.8	0.88	−3.7	16.1	0.97 *	9.2	0.84	0.97 *
LDH-Ibu/Alg, 0.5 g L^{-1}	PBS	12.6	4.8	0.85	2.0	16.3	0.96	16.9	0.54	0.98 *
Ibu/Alg		9.9	4.2	0.88	0.8	14.3	0.98	14.1	0.54	0.99
LDH-Ibu/Alg, 5 g L^{-1}		1.5	2.4	0.98	−3.0	7.7	0.98	4.2	0.73	0.99 *
LDH-Ibu/Alg, 0.5 g L^{-1}	SBF	8.6	3.6	0.90	1.0	11.9	0.98 *	12.8	0.48	0.98 *
Ibu/Alg		17.0	3.3	0.86	9.8	11.2	0.97	21.8	0.30	0.99 *
LDH-Nap/Alg, 5 g L^{-1}		17.0	5.2	0.69	4.1	18.5	0.86 *	16.1	0.74	0.87 *
LDH-Nap/Alg, 0.5 g L^{-1}	PBS	12.0	6.1	0.89	−1.1	20.5	0.98 *	17.4	0.62	0.98 *
Nap/Alg		11.1	5.3	0.90	−0.23	18.0	0.99 *	16.3	0.58	0.99 *
LDH-Nap/Alg, 5 g L^{-1}		4.1	4.7	0.97	−5.0	15.2	0.99 *	9.0	0.73	0.99 *
LDH-Nap/Alg, 0.5 g L^{-1}	SBF	12.5	4.5	0.91	2.9	15.2	0.99 *	18.5	0.42	0.97
Nap/Alg		15.5	5.0	0.90	4.8	17.0	0.99 *	22.0	0.42	0.99 *

k_0, k_H and k_P expressed as % h^{-1}, % h$^{-0.5}$ and % h^{-n}, respectively. The concentration of pure drug experiments was calculated to match that of the 0.5 g L^{-1} LDH-Drug/Alg dispersions.

Release profiles in the SBF of both drugs were more influenced by their inclusion in LDH layers, with the release from both 0.5 and 5 g L^{-1} LDH-Drug/Alg being increasingly slower than that of Drug/Alg. Significant differences were observed in release profiles ($f_1 > 27$ when comparing Drug/Alg and 0.5 g L^{-1} LDH-Drug/Alg; $f_1 = 54$ and $f_2 = 48$ when comparing 0.5 and 5 g L^{-1} LDH-Drug/Alg). Nevertheless, and similarly to that observed in the PBS medium, the best fits were obtained with the K-P model (Table 2), with *n* values near 0.5 for all Drug/Alg and 0.5 g L^{-1} LDH-Drug/Alg and, in agreement, good fittings were also obtained with the Higuchi model. These results indicated that a diffusion-controlled mechanism was again controlling the drug release. In the case of 5 g L^{-1} LDH-Drug/Alg, the *n* values of K-P model increased (0.73 and 0.84 for Ibu and Nap, respectively), which indicated an anomalous behavior, like that produced towards PBS. Then, the mechanism of drug release was not so different in both media, and the main difference was the release rate, which decreased with increasing LDH–drug concentration. The cumulative drug release at the end of the assay reached 39, 32 and 19% for Ibu/Alg, 0.5 and 5 g L^{-1} LDH-Ibu/Alg, respectively, while 49, 44 and 39% were achieved for Nap-containing samples. This effect was more pronounced in the release from LDH-Ibu/Alg than for LDH-Nap/Alg, as corresponds to the above-mentioned affinity of Ibu$^-$ anions for the LDH interlayers.

The differences in the release profiles toward SBF compared to PBS were assigned to Alg gelation when exposed to the divalent calcium ions present in the SBF. This Ca-Alg gel included and fixed the LDH–drug particles, which crosslinked the Alg chains and performed as barrier for drug diffusion, decreasing the overall release rate. Effectively, a consistent gel, which was easily separated from the acetate cellulose membrane, was formed in the donor compartment of the Franz cells (not shown). This in-situ gel formation presents promising applications in tissue engineering [43]. This gel formation will also ease the fixation of the biomaterial to the insertion place and locate the action of loaded drug, which would be released in a controlled manner.

3.4. Cell Proliferation Assay

Biomaterials for bone regeneration must provide support for cell adhesion and proliferation, which can be compromised by cytotoxic effects caused by the inclusion of drugs such as Ibu and Nap. To explore the capacity of LDH to diminish these cytotoxic effects, the proliferation of pre-osteoblastic MC3T3-E1 cells in the presence of LDH-Drug/Alg dispersions was determined (Figure 5). Experiments with LDH-Cl, Alg and their mixture (LDH-Cl/Alg), as well as in the presence of the pure drugs, the LDH–drug particles, and Drug/Alg dispersions were also performed to differentiate between factors of their overall behavior.
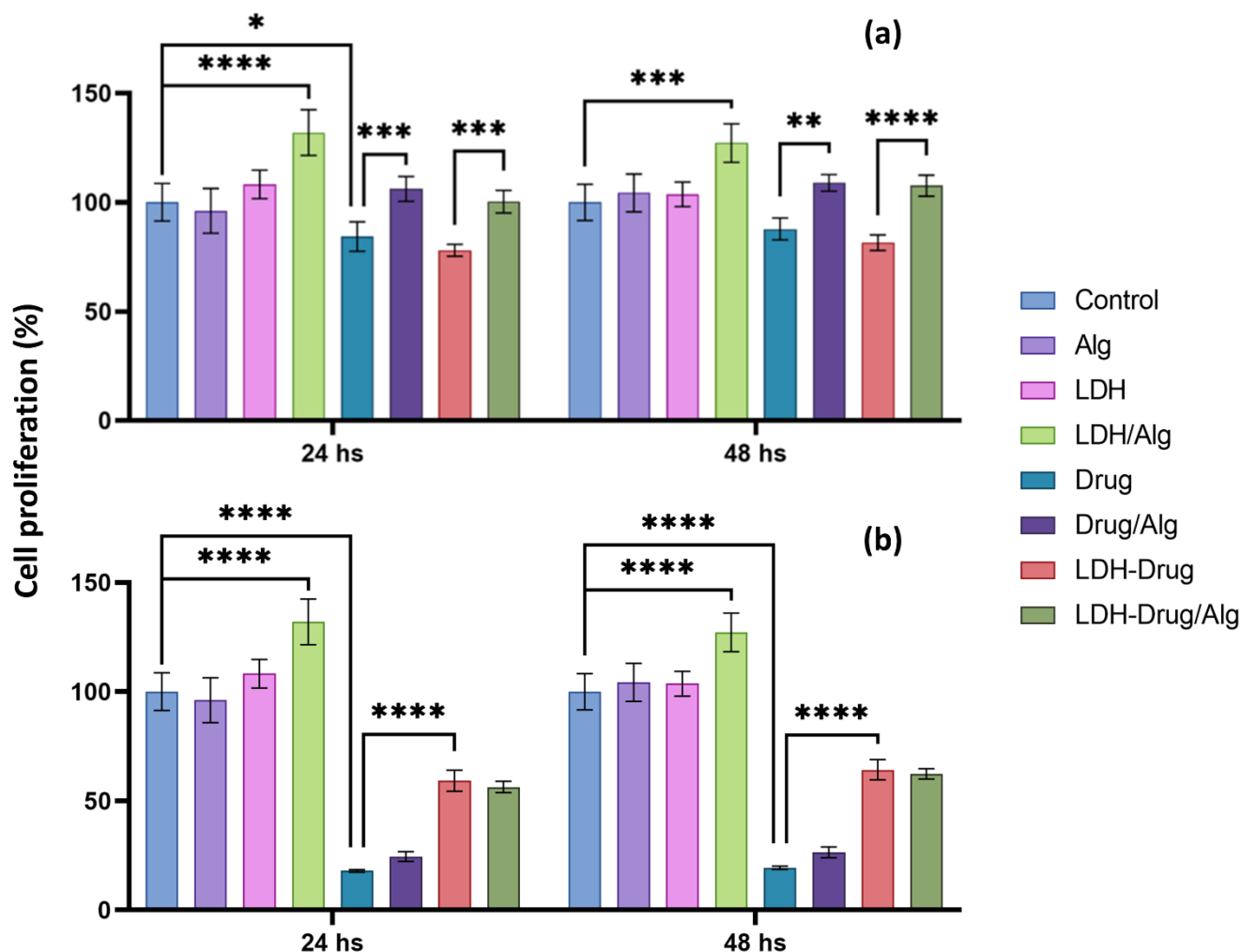

Figure 5. Anti-cytotoxic effect of 5 g L^{-1} LDH-Drug/Alg in MC3T3-E1 cell cultures. Proliferation of MC3T3-E1 cells cultured in CM (control), Alg, LDH, LDH/Alg, Drug (Ibu (**a**) and Nap (**b**)), Drug/Alg, LDH-Drug, LDH-Drug/Alg. Fluorescence of alamarBlue was measured at 24 and 48 h of and expressed as a percentage of control proliferation at that given time. Asterisks indicate significant differences between the indicated groups (****, $p < 0.0001$, ***, $p < 0.001$, **, $p < 0.01$ and *, $p < 0.05$).

In the absence of the drug, the separate presence of Alg or LDH-Cl did not produce significant differences in the proliferation of MC3T3-E1 cells compared to the control, which was in line with the low cytotoxicity of both materials [12,44]. Although LDH layers did not interfere with cell adhesion and proliferation, they have been proposed to have a positive effect on biomaterials such as polycaprolactone [45]. Comparable results were obtained for LDH-Cl/Alg, which produced a significant increase in cell activity ($p < 0.001$), which was related to the hydrophilicity and positive charge of the LDH surface, providing attachment sites due to electrostatic interactions with negatively charged cell membranes [12]. The

presence of pure drugs decreased the percentage of cell proliferation compared to the control, with a reduction of approximately 81% and 13% for Nap ($p < 0.0001$) and Ibu, respectively, after 48 h, although the latter decrease was not considered significant according to ANOVA analysis. The cytotoxic effect of Ibu was significantly reduced when cultivated in the Alg matrix, showing an increase in proliferation of 24% compared to the pure drug ($p < 0.01$), while, in the case of Nap, the polymeric matrix did not significantly enhance the cell proliferation. On the other hand, the inclusion of Ibu in LDH did not show significant differences in cell proliferation compared to the pure drug, which was assigned to the low cytotoxicity of the drug, as well as the negative charge and hydrophobicity of the LDH-Ibu surface, while LDH-Nap reduced in 55% the cytotoxic effect of the pure drug ($p < 0.0001$). The results for the LDH-Drug/Alg dispersions were consistent with the previously exposed trends, as they showed a cellular protection that was dependent on the intercalated drug. In the case of Ibu, a significantly increased proliferation was obtained compared to pure Ibu and LDH-Ibu due to the protective action of Alg ($p < 0.001$). Instead, the LDH-Nap/Alg dispersion showed a highly significant anticytotoxic effect, like that of the LDH-Nap dispersion, which indicated that its inclusion in the LDH structure is mainly responsible for the protective effect ($p < 0.0001$). Therefore, LDH-Drug/Alg dispersions are a promising and versatile biomaterial for cell culturing that, depending on the physicochemical properties and composition of the included LDH, can provide cell adhesion centers and/or cytoprotective effects. This strategy can be extended to drugs that provide antimicrobial and anticancer properties of cell differentiation to biomaterials for tissue engineering applications.

4. Conclusions

In this work, the physicochemical properties of LDH/Alg dispersions were explored, aiming at their application in tissue engineering. LDH intercalated with Ibu and Nap were obtained and incorporated in Alg dispersions, with significant effects in their surface charge but minor effects on their aggregation. The sterilization of dispersions by TT did not produce significant changes in the aggregate size of LDH–drug particles. The drug release behavior was highly dependent on the release media, and particularly to the presence of Ca^{2+} ions present in the SBF. The formation of a gel layer upon exposure to SBF led to a release rate diminution with increasing LDH concentration. The main release mechanism was drug diffusion through the LDH/Alg dispersions, although anion exchange also influenced the overall rate at high LDH concentrations. Finally, LDH/Alg dispersions had a protective effect against the cytotoxic effects of drugs in cell culture. This protective effect was provided by Alg or LDH depending on the intercalated drug. LDH/Alg dispersions are then promising biomaterials for tissue engineering due to their capacity to provide drug release control and cell proliferation enhancement and/or protection. These dispersions can be included in scaffold formulations on their own, due to their in-situ gelling capacity, and can also be used, for example, as precursors of biomaterials gelled by ionic crosslinking with Ca^{2+} ions or lyophilized for subsequent rehydration with solutions containing stem cells or bone marrow aspirates.

Author Contributions: Conceptualization, R.R.; methodology, R.R., M.C.G., G.A.G.; validation, M.C.G., G.A.G.; formal analysis, R.R., M.C.G., G.A.G.; data curation, J.P.Z.; investigation, R.R., M.C.G., J.P.Z.; writing—original draft preparation, R.R., M.C.G., G.A.G., J.P.Z.; writing—review and editing, R.R., M.C.G.; visualization, R.R., M.C.G., J.P.Z.; supervision, R.R., M.C.G., G.A.G.; project administration, R.R.; funding acquisition, R.R., M.C.G., G.A.G. All authors have read and agreed to the published version of the manuscript.

Córdoba (MinCyT, Cordoba Innova Program). The SEM images were obtained at the Laboratorio de Microscopía Electrónica y Análisis por Rayos X (LAMARX).

Conflicts of Interest: The authors declare no conflict of interest.

References

1. Hariyadi, D.M.; Islam, N. Current status of alginate in drug delivery. *Adv. Pharmacol. Pharm. Sci.* **2020**, *2020*, 8886095. [CrossRef] [PubMed]
2. Ray, P.; Maity, M.; Barik, H.; Sahoo, G.S.; Hasnain, M.S.; Hoda, M.N.; Nayak, A.K. Alginate-based hydrogels for drug delivery applications. In *Alginates in Drug Delivery*; Academic Press: Cambridge, MA, USA, 2020. [CrossRef]
3. Venkatesan, J.; Bhatnagar, I.; Manivasagan, P.; Kang, K.H.; Kim, S.K. Alginate composites for bone tissue engineering: A review. *Int. J. Biol. Macromol.* **2015**, *72*, 269–281. [CrossRef] [PubMed]
4. Sotome, S.; Uemura, T.; Kikuchi, M.; Chen, J.; Itoh, S.; Tanaka, J.; Tateishi, T.; Shinomiya, K. Synthesis and in vivo evaluation of a novel hydroxyapatite/collagen- alginate as a bone filler and a drug delivery carrier of bone morphogenetic protein. *Mater. Sci. Eng. C* **2004**, *24*, 341–347. [CrossRef]
5. Frankenberg, E. Controlled nucleation of hydroxyapatite on alginate scaffolds for stem cell-based bone tissue engineering. *Bone* **2012**, *23*, 1–7. [CrossRef]
6. Axpe, E.; Oyen, M.L. Applications of alginate-based bioinks in 3D bioprinting. *Int. J. Mol. Sci.* **2016**, *17*, 1976. [CrossRef]
7. Alcantara, A.C.S.; Aranda, P.; Darder, M.; Ruiz-Hitzky, E. Bionanocomposites based on alginate-zein/layered double hydroxide materials as drug delivery systems. *J. Mater. Chem.* **2010**, *20*, 9495–9504. [CrossRef]
8. Hasnain, M.S.; Ahmed, S.A.; Behera, A.; Alkahtani, S.; Nayak, A.K. Inorganic materials–alginate composites in drug delivery. In *Alginates in Drug Delivery*; Academic Press: Cambridge, MA, USA, 2020. [CrossRef]
9. Song, F.; Li, X.; Wang, Q.; Liao, L.; Zhang, C. Nanocomposite hydrogels and their applications in drug delivery and tissue engineering. *J. Biomed. Nanotechnol.* **2015**, *11*, 40–52. [CrossRef]
10. Rives, V. *Layered Double Hydroxides: Present and Future*; Nova Publishers: Hauppauge, NY, USA, 2001.
11. Izbudak, B.; Cecen, B.; Anaya, I.; Miri, A.K.; Bal-Ozturk, A.; Karaoz, E. Layered double hydroxide-based nanocomposite scaffolds in tissue engineering applications. *RSC Adv.* **2021**, *11*, 30237–30252. [CrossRef]
12. Rojas, R.; Mosconi, G.; Pablo, J.; Gil, G.A. Layered double hydroxide applications in biomedical implants. *Appl. Clay Sci.* **2022**, *224*, 106514. [CrossRef]
13. Rives, V.; del Arco, M.; Martín, C. Layered double hydroxides as drug carriers and for controlled release of non-steroidal antiinflammatory drugs (NSAIDs): A review. *J. Control. Release* **2013**, *169*, 28–39. [CrossRef]
14. Rojas, R.; Jimenez-Kairuz, A.F.; Manzo, R.H.; Giacomelli, C.E. Release kinetics from LDH-drug hybrids: Effect of layers stacking and drug solubility and polarity. *Colloids Surf. A Physicochem. Eng. Asp.* **2014**, *463*, 37–43. [CrossRef]
15. Szabados, M.; Gácsi, A.; Gulyás, Y.; Kónya, Z.; Kukovecz, Á.; Csányi, E.; Pálinkó, I.; Sipos, P. Conventional or mechanochemically-aided intercalation of diclofenac and naproxen anions into the interlamellar space of CaFe-layered double hydroxides and their application as dermal drug delivery systems. *Appl. Clay Sci.* **2021**, *212*, 106233. [CrossRef]
16. Bernardo, M.P.; Rodrigues, B.C.S.; de Olivera, T.D.; Guedes, A.P.M.; Batista, A.A.; Mattoso, L.H.C. Naproxen/layered double hydroxide composites for tissue-engineering applications: Physicochemical characterization and biological evaluation. *Clays Clay Miner.* **2020**, *68*, 623–631. Available online: https://link.springer.com/article/10.1007/s42860-020-00101-w (accessed on 22 February 2022). [CrossRef]
17. Yousefi, Y.; Tarhriz, V.; Eyvazi, S.; Dilmaghani, A. Synthesis and application of magnetic@layered double hydroxide as an anti-inflammatory drugs nanocarrier. *J. Nanobiotechnol.* **2020**, *18*, 155. [CrossRef]
18. Kang, H.; Shu, Y.; Li, Z.; Guan, B.; Peng, S.; Huang, Y.; Liu, R. An effect of alginate on the stability of LDH nanosheets in aqueous solution and preparation of alginate/LDH nanocomposites. *Carbohydr. Polym.* **2014**, *100*, 158–165. [CrossRef]
19. Vasti, C.; Borgiallo, A.; Giacomelli, C.E.; Rojas, R. Layered double hydroxide nanoparticles customization by polyelectrolyte adsorption: Mechanism and effect on particle aggregation. *Colloids Surf. A Physicochem. Eng. Asp.* **2017**, *533*, 316–322. [CrossRef]
20. Borgiallo, A.; Rojas, R. Reactivity and Heavy Metal Removal Capacity of Calcium Alginate Beads Loaded with Ca–Al Layered Double Hydroxides. *ChemEngineering* **2019**, *3*, 22. [CrossRef]
21. Zhang, J.P.; Wang, Q.; Xie, X.L.; Li, X.; Wang, A.Q. Preparation and swelling properties of pH-sensitive sodium alginate/layered double hydroxides hybrid beads for controlled release of diclofenac sodium. *J. Biomed. Mater. Res. Part B Appl. Biomater.* **2010**, *92*, 205–214. [CrossRef]
22. Viscusi, G.; Gorrasi, G. Facile preparation of layered double hydroxide (LDH)-alginate beads as sustainable system for the triggered release of diclofenac: Effect of pH and temperature on release rate. *Int. J. Biol. Macromol.* **2021**, *184*, 271–281. [CrossRef]

23. Munhoz, D.R.; Bernardo, M.P.; Malafatti, J.O.D.; Moreira, F.K.V.; Mattoso, L.H.C. Alginate films functionalized with silver sulfadiazine-loaded [Mg-Al] layered double hydroxide as antimicrobial wound dressing. *Int. J. Biol. Macromol.* **2019**, *141*, 504–510. [CrossRef]

24. U.S. Pharmacopoeial Convention. *United States Pharmacopoeia*; U.S. Pharmacopoeial Convention: Rockville, MD, USA, 2015.

25. Marques, M.R.C.; Loebenberg, R.; Almukainzi, M. Simulated biological fluids with possible application in dissolution testing. *Dissolut. Technol.* **2011**, *18*, 15–28. [CrossRef]

26. Costa, P.; Sousa Lobo, J.M. Modeling and comparison of dissolution profiles. *Eur. J. Pharm. Sci.* **2001**, *13*, 123–133. [CrossRef]

27. Castellaro, A.M.; Rodriguez-Baili, M.C.; Di Tada, C.E.; Gil, G.A. Tumor-associated macrophages induce endocrine therapy resistance in ER+ breast cancer cells. *Cancers* **2019**, *11*, 189. [CrossRef] [PubMed]

28. Drits, V.A.; Bookin, A.S. Crystal Structure and X-ray identification of Layered Double hydroxides. In *Layered Double Hydroxides: Present and Future*; Rives, V., Ed.; Nova Science: Hauppauge, NY, USA, 2001; pp. 39–92.

29. Mohanambe, L.; Vasudevan, S. Anionic clays containing anti-inflammatory drug molecules: Comparison of molecular dynamics simulation and measurements. *J. Phys. Chem. B* **2005**, *109*, 15651–15658. [CrossRef]

30. Gu, Z.; Wu, A.; Li, L.; Xu, Z.P. Influence of hydrothermal treatment on physicochemical properties and drug release of anti-inflammatory drugs of intercalated layered double hydroxide nanoparticles. *Pharmaceutics* **2014**, *6*, 235–248. [CrossRef]

31. Figueiredo, M.P.; Cunha, V.R.R.; Cellier, J.; Taviot-Guého, C.; Constantino, V.R.L. Fe(III)-Based Layered Double Hydroxides Carrying Model Naproxenate Anions: Compositional and Structural Aspects. *ChemistrySelect* **2022**, *7*, e202103880. [CrossRef]

32. Kloprogge, J.T.; Frost, R.L. Infrared and Raman Spectroscopic Studies of Layered Double Hydroxides (LDHs). In *Layered Double Hydroxides: Present and Future*; Rives, V., Ed.; Nova Science Publishers: Hauppauge, NY, USA, 2001; pp. 139–192.

33. Gaskell, E.E.; Ha, T.; Hamilton, A.R. Ibuprofen intercalation and release from different layered double hydroxides. *Ther. Deliv.* **2018**, *9*, 653–666. [CrossRef]

34. Wypych, F.; Arízaga, G.G.C.; da Costa Gardolinski, J.E.F. Intercalation and functionalization of zinc hydroxide nitrate with mono- and dicarboxylic acids. *J. Colloid Interface Sci.* **2005**, *283*, 130–138. [CrossRef]

35. Rojas, R.; Palena, M.C.; Jimenez-Kairuz, A.F.; Manzo, R.H.; Giacomelli, C.E. Modeling drug release from a layered double hydroxide-ibuprofen complex. *Appl. Clay Sci.* **2012**, *62–63*, 15–20. [CrossRef]

36. Luengo, C.V.; Crescitelli, M.C.; Lopez, N.A.; Avena, M.J. Synthesis of Layered Double Hydroxides Intercalated With Drugs for Controlled Release: Successful Intercalation of Ibuprofen and Failed Intercalation of Paracetamol. *J. Pharm. Sci.* **2021**, *110*, 1779–1787. [CrossRef]

37. Du, B.-Z.; Wang, R.M. Synthesis and characterizations of naproxen intercalated Mg-Al layered double hydroxides. *J. Chin. Pharm. Sci.* **2010**, *19*, 371–378.

38. Rojas, R.; Linck, Y.G.; Cuffini, S.L.; Monti, G.A.; Giacomelli, C.E. Structural and physicochemical aspects of drug release from layered double hydroxides and layered hydroxide salts. *Appl. Clay Sci.* **2015**, *109–110*, 119–126. [CrossRef]

39. Rojas Delgado, R.; Arandigoyen Vidaurre, M.; de Pauli, C.P.; Ulibarri, M.A.; Avena, M.J. Surface-charging behavior of Zn-Cr layered double hydroxide. *J. Colloid Interface Sci.* **2004**, *280*, 431–441. [CrossRef]

40. Rojas, R.; Barriga, C.; de Pauli, C.P.; Avena, M.J. Influence of carbonate intercalation in the surface-charging behavior of Zn–Cr layered double hydroxides. *Mater. Chem. Phys.* **2010**, *119*, 303–308. [CrossRef]

41. Pavlovic, M.; Rouster, P.; Oncsik, T.; Szilagyi, I. Tuning Colloidal Stability of Layered Double Hydroxides: From Monovalent Ions to Polyelectrolytes. *ChemPlusChem* **2017**, *82*, 121–131. [CrossRef]

42. Vasti, C.; Giacomelli, C.E.; Rojas, R. Pros and cons of coating layered double hydroxide nanoparticles with polyacrylate. *Appl. Clay Sci.* **2019**, *172*, 11–18. [CrossRef]

43. Baino, F.; Yamaguchi, S. The use of simulated body fluid (SBF) for assessing materials bioactivity in the context of tissue engineering: Review and challenges. *Biomimetics* **2020**, *5*, 57. [CrossRef]

44. Lee, K.Y.; Mooney, D.J. Alginate: Properties and biomedical applications. *Prog. Polym. Sci.* **2012**, *37*, 106–126. [CrossRef]

45. Baradaran, T.; Shafiei, S.S.; Mohammadi, S.; Moztarzadeh, F. Poly (ε-caprolactone)/layered double hydroxide microspheres-aggregated nanocomposite scaffold for osteogenic differentiation of mesenchymal stem cell. *Mater. Today Commun.* **2020**, *23*, 100913. [CrossRef]